Q^n distribution in stoichiometric silicate glasses: thermodynamic calculations and ^{29}Si high resolution NMR measurements

J. Schneider [a,*], V.R. Mastelaro [a], E.D. Zanotto [b], Boris A. Shakhmatkin [c], Natalia M. Vedishcheva [c], Adrian C. Wright [d], H. Panepucci [a]

[a] *IFSC Universidade de São Paulo, Avenida Trabalhador São-Carlense 400, Centro, CEP 13566-590 São Carlos, SP, Brazil*
[b] *Vitreous Materials Laboratory, Department of Materials Engineering, Federal University of São Carlos, 13565-905 São Carlos, SP, Brazil*
[c] *Institute of Silicate Chemistry of the Russian Academy of Sciences, Ul. Odoevskogo, 24, Korp. 2, St. Petersburg 199155, Russia*
[d] *J.J. Thomson Physical Laboratory, University of Reading, Whiteknights, Reading RG6 6AF, UK*

Received 19 September 2002

Abstract

To test the validity of a thermodynamic model (TM) for glass structure (model of associated solutions previously proposed by some of us) the distributions of silicon species Q^n in several stoichiometric glasses were estimated by nuclear magnetic resonance. The following glasses were considered: $CaO \cdot SiO_2$ (CS), $BaO \cdot 2SiO_2$ (BS2), $Na_2O \cdot 2CaO \cdot 3SiO_2$ ($1 \cdot 2 \cdot 3$), $2Na_2O \cdot CaO \cdot 3SiO_2$ ($2 \cdot 1 \cdot 3$), $CaO \cdot MgO \cdot 2SiO_2$ (CMS2) and $PbO \cdot SiO_2$ (PS). In contrast to the usual assumption that all kinds of Q^n species can be present in the glass structure, the basic hypothesis of the TM limits the possible set of species in the glass to those effectively observed in the crystalline phases of the equilibrium phase diagram. The Q^n distributions for the set of glasses were calculated at temperatures close to the respective glass transition temperatures. A satisfactory agreement was found between the predicted and experimental Q^n populations for glasses $1 \cdot 2 \cdot 3$, BS2 and $2 \cdot 1 \cdot 3$. On the other hand, for glasses CS, CSM2 and PS, agreement between experiment and model results is obtained assuming that the expected amount of Q^4 silicon in the glass is organized in silica-like domains of molecular size, having Q^3 units at their 'interfaces'.
© 2003 Elsevier B.V. All rights reserved.

PACS: 61.43.F; 76.60; 65.50

1. Introduction

A detailed experimental study of any property, as a function of composition in multi-component systems, typically requires a large number of experiments. That is why the modeling of properties of glasses and melts is a compelling problem. An

*Corresponding author. Tel.: + 55-16 273 9600; fax:+55-16 273 9876.

E-mail address: schnei@if.sc.usp.br (J. Schneider).

ideal model must be predictive (i.e. it must avoid adjustable parameters) over extended composition, temperature and pressure regions, for systems formed from any number of components, and has to provide the possibility of calculating a wide variety of properties. The results for a given system should be in agreement with available information on its structure.

In a series of previous papers [1–8], it has been shown that the thermodynamic model (TM) of associated solutions meets the above requirements for oxide glasses and melts, formed from distinct chemical components. The model uses only the standard Gibbs free energies of formation of crystalline compounds, tabulated for various binary and ternary systems, as input parameters. It yields an adequate description of the entire set of thermodynamic potentials of systems formed from any number of components [1–3]. In addition, due to the fact that a wide range of physical properties of glasses and melts are the derivatives of the Gibbs free energy with respect to different variables of state, this TM enables these properties to be calculated [2–5]. Finally, the model relates the thermodynamic potentials to specific atomic interactions and the distribution of various structural units which determine the short-range and, to a certain extent, the medium-range order in glasses and melts [2,3,6–8]. In this work, model predictions of the short-range order in silicate glasses are being tested using the results of high resolution ^{29}Si-nuclear magnetic resonance (NMR) experiments.

2. The model of associated solutions

When in contact, basic and acidic oxides interact (especially at high temperatures and, sometimes, even at room temperature) and, similar to the interaction between a base and an acid, they form salt-like products (silicates, borates, germanates, etc.). An adequate model has to take into account these processes. Thus, approximately twenty models are known, which are used to describe the properties of oxide systems on the basis of various structural concepts. All of these models need to use experimental thermodynamic data for

melts and/or glasses. The model of associated solutions [2] considered here is based on the rigorous thermodynamic theory of affinity of De Donder and Van Rysselberghe [9] and describes the thermodynamic properties of homogeneous systems formed from any number of components at any temperature.

The basis of the model is that a melt, formed from components with different chemical nature, is considered as a medium where chemical reactions proceed in the direction of the equilibrium state. These reactions are characterized by their standard Gibbs free energies, which are the parameters determining the actual equilibrium composition (this concept is explained below). On achieving the equilibrium state, the Gibbs free energy of a system is a minimum. Thus, the suggested approach is an extension of the applicability of equation of the van't Hoff isotherm to the case of several reactions proceeding simultaneously.

The probability of chemical reactions and the possibility of calculating their standard Gibbs free energies (ΔG_r^0) are totally independent of the state of aggregation of initial reagents and final products, as well as of the nature of their chemical bonds (ionic, covalent, etc.). It should be noted that only the equilibrium state of a system is considered here. Thus, within the framework of the model, oxide melts are considered as an equilibrium solution formed from unreacted initial oxides and the salt-like products of their interaction. These salt-like products represent structural chemical groupings of definite composition, with similar stoichiometry to that of the crystalline compounds shown by the equilibrium phase diagram of the system considered. According to recent structural data [10], a structural similarity between the salt-like groupings and crystals of the same stoichiometry can also be assumed, at least with respect to the ratio between the basic structural units (boron–oxygen and silicon–oxygen polyhedra).

At high temperatures (above 1000 °C for alkali-silicate, borate and germanate systems), it is possible to neglect deviations from the ideal behaviour of a system that are due to the difference in size and shape of the unreacted initial oxides and the salt-like groupings. In this case, a single-phase

system can be described on the basis of the ideal approximation of the model. This implies that the salt-like groupings and the unreacted oxides form an ideal solution. Hence, the energy of the system is independent of the specific type of groupings that surround a given grouping or, in other words, it is assumed that the groupings are statistically distributed in space. As shown in Ref. [1], this approximation is valid for a wide variety of systems that present a basis for many industrial glasses.

The mathematical formalism of the model of associated solutions consists of a search for a minimum in the Gibbs free energy of a system as a function of the degree of completeness of reactions. As shown in Ref. [11, p. 141], this corresponds to the solution of a system of equations for the law of mass balance of the components and those describing the law of mass action for all of the reactions that proceed in the system of a given composition (if required, the expressions for the excess Gibbs free energy of mixing of the salt-like products are taken into account). Examples of such systems of equations are given in Refs. [2,5,12]. The solution of these systems provides information on the equilibrium composition of the glass (melt), which allows its chemical structure to be determined. The notion of the chemical structure of glasses implies the content in them of the salt-like products (groupings) and the unreacted initial oxides. This content can be represented by the number of moles (n_i) or by the mole fractions (X_i) of all of the species. The relationship between them is determined by the formula

$$X_i = n_i / \sum n_i.$$

It should be noted that the symbol n_i represents the absolute value of the number of moles that form in the course of the interaction between X^* moles of Na_2O and $(1 - X^*)$ moles of SiO_2, B_2O_3, etc. while the symbol X_i represents the values referred to a new total sum of all of the chemical species (salt-like groupings) present in the system, due to the achievement of the equilibria of the reactions that proceed in the system. Thus, a transformation can be made to new concentration co-ordinates that describe the system (see for example Ref. [13, p. 387]). These new concentrations

are called actual co-ordinates or actual concentrations as opposed to analytical concentrations.

It should be stressed that, as follows from calculations made for a wide variety of glasses and melts, there is no single set of salt-like species that is common for all glass-forming systems of a given type. In each particular case, this set has to be determined on the basis of information from the phase diagram of the given system, followed by an analysis of the thermodynamic stability of the relevant compounds. The idea of a certain set of species, which is unique for a range of borate, silicate or other systems, can lead to serious mistakes such as the misinterpretation of structural data obtained by various experimental techniques. As an example, Fig. 1(a) and (b) shows the chemical structure of sodium silicate melts, at various temperatures, over the composition region from 0 to 60 mol% Na_2O. The salt-like species present in these melts are similar in their stoichi-

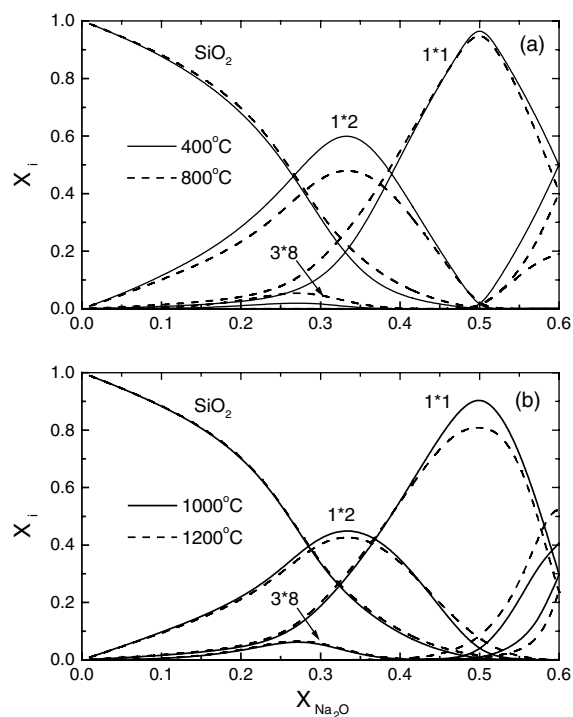Fig. 1. Chemical structure ($mNa_2O \cdot nSiO_2$) of sodium silicate melts at various temperatures, over the composition region from 0 to 60 mol% Na_2O. (a) Solid line: 400 °C. Dashed line: 800 °C. (b) Solid line: 1000 °C. Dashed line: 1200 °C.

ometry to the crystalline compounds that are shown in the phase diagram of the system Na_2O–SiO_2 [14].

A knowledge of the chemical structure of a given glass, together with information on the structure of the stoichiometric crystalline compounds that form in the relevant system, allows the distribution of the basic structural units in glasses to be calculated. In the case when the crystal structures are unknown, the distribution of various X–oxygen (X = Si, B, Ge, P) polyhedra in glasses can be modeled, with a certain degree of accuracy, if it is known how the structure of a vitreous network changes on addition of modifying oxides, i.e. whether X–O bonds form or are broken due to the introduction of each new metal atom. Examples of modeling the concentration and temperature distribution of the basic structural units in borate and binary/ternary silicate glasses and melts are given in Refs. [2,3,6–8,15].

3. Experimental

The glasses were prepared by melting homogeneous mixtures of analytical grade reagents in 100-ml Pt crucibles, in electric furnaces. The melting temperatures ranged from 1450 to 1550 °C, with a hold time of about two hours. To avoid crystallization, the melts were cast between cold steel plates and manually pressed at estimated cooling rates between 100 and 500 °C/s. Additional details concerning the preparation of the glasses can be found in Ref. [16].

High resolution ^{29}Si-NMR spectra were obtained in a magnetic field of 9.4 T, at a frequency of 79.45 MHz, with a Varian Unity Inova spectrometer. Measurements were carried out under magic-angle sample spinning (MAS) of up to 6 kHz, using a 7 mm wide-body CP/MAS probe from Varian and 7 mm zirconia rotors. The spectra were obtained from free induction decay signals after $\pi/2$ pulses of 4 µs length. Relatively long recycle times were used to avoid any possible effects of differential relaxation across the inhomogeneously broadened NMR line. For each glass, it was verified that the pulse recycling time was long enough to avoid saturation, resulting in recycling

times up to 400 s. A polycrystalline kaolinite sample was used as secondary external standard for referencing chemical shifts (−91.2 ppm with respect to tetrametilsilane, TMS).

The population of Q^n silicon sites was estimated from a least squares fitting of the spectra, assuming Gaussian distributions of isotropic chemical shifts δ_{ISO} for each type of Q^n unit. For broad NMR lines, the overlapping of Q^n resonances gives raise to co-variances between best-fit intensity parameters, this being a source of uncertainty for the Q^n populations. To minimize this effect, several physical criteria were imposed on the fitting procedure to discard unrealistic numerical results. Thus, full width at half maximum (FWHM) values of individual Gaussians were restricted to less than 15 ppm, based on the chemical shifts observed in different crystalline silicates [17]. Each non-bridging oxygen atom (NBO) produces a deshielding of between 5 and 10 ppm with respect to the chemical shift of a Q^4 silicon in a silica-like environment. Therefore, the centers of adjacent Gaussians attributed to Q^n and Q^{n+1} units should be separated by more than 5 ppm. The number of Gaussians used in each case was determined by the overall chemical shift range spanned by the NMR spectrum and other spectral features, such as partially resolved bumps or asymmetries. With these criteria, up to four partially overlapped Gaussian distributions were needed to deconvolute the spectra. In some cases, equally acceptable fits were obtained from deconvolutions with three and four Gaussian functions. To choose physically significant fits, stoichiometric criteria and literature data for isotropic chemical shifts were considered. For alkali and alkaline-earth metasilicate glasses, the values for the intensities resulting from the fitting procedure described above were compatible with the stoichiometric condition $2Q^0 + Q^1 = Q^3 + 2Q^4$ within the uncertainty of the method.

4. Results

4.1. Thermodynamic modeling

An analysis of the agreement between the NMR measurements and the model prediction of Q^n

values should commence with estimating the uncertainty in the modeling. According to the formalism of the model used, the accuracy of calculating the distribution of the basic structural units in glasses depends on the accuracy of the determination of their chemical structure. In Ref. [5], it is shown that the chemical structure is calculated with an error entirely determined by the reliability of the standard Gibbs free energies of formation, ΔG_f^0, from the oxides of the compounds existing in the particular system. Fig. 2 shows the change in the fractions of Q^n species in sodium silicate melts, at 1200 °C, due to a variation of ±1 kcal/mol in the potentials, ΔG_f^0, calculated according to the reaction

$$m\text{Na}_2\text{O} + n\text{SiO}_2 = m\text{Na}_2\text{O} \cdot n\text{SiO}_2,$$
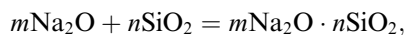
from the data reported in Ref. [18] for the sodium silicate compounds and the constituent oxides. It is seen that the maximum change, which is observed for the case of Q^1 and Q^2 species, does not exceed 0.1. Note that, in general, the potentials ΔG_f^0 used in the model calculations are chosen on the basis of a critical analysis of the available literature data. From the thermodynamic data reported in Refs. [18–21], it follows that, for the compositions considered in this paper, the uncertainty in the ΔG_f^0 values used in the model calculations is less

than ±1 kcal/mol. Therefore, it can be expected that the Q^n values listed in Tables 1 and 2, respectively, for alkali-silicate and alkaline-earth

Table 1
Populations of silicon species in several binary alkali-silicate glasses calculated with the TM

Glass	Q^0	Q^1	Q^2	Q^3	Q^4
Li₂O · 2SiO₂					
Population (NMR) [%][a]			10	63	22
Population (NMR) [%][b]			14.5	71	14.5
Population (TM) [%]	0.002		25.6	48.9	25.61
Li₂O · SiO₂					
Population (NMR) [%][b]		8.5	83	8.5	
Population (TM) [%]	1.3		96.4	1.9	0.3
Na₂O · SiO₂					
Population (NMR) [%][a]	1	13	70	16	
Population (NMR) [%][b]	1	7.5	85	7.5	
Population (TM) [%]	0.35	9.70	79.82	9.86	0.27
K₂O · SiO₂					
Population (NMR) [%][b]		2	96	2	
Population (NMR) [%][a]		7	84	9	
Population (TM) [%]	1.4		95.8	2.7	0.1
Na₂O · 2SiO₂					
Population (NMR) [%][a]			10	79	11
Population (NMR) [%][b]			7.5	85	7.5
Population (TM) [%]			12.0	75.9	12.1
K₂O · 2SiO₂					
Population (NMR) [%][a]			7	86	7
Population (NMR) [%][a]			5.5	89	5.5
Population (TM) [%]			1.3	97.3	1.4

Experimental NMR data were taken from literature.
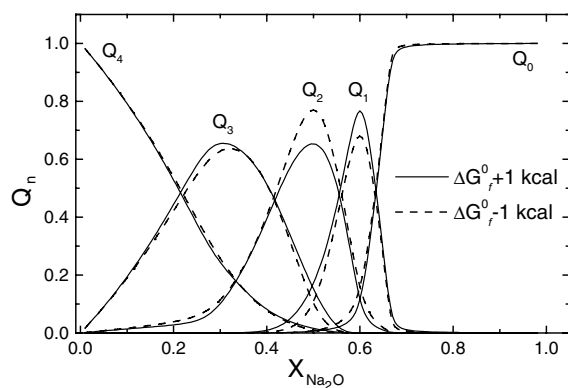[a] Ref. [30].
[b] Ref. [31].

Fig. 2. Evaluation of the variation in calculated fractions of Q^n species in sodium silicate melts due to a variation on the Gibbs free-energies ΔG_f^0 of the oxides in ±1 kcal around the experimental values (Ref. [18]). Calculations were carried out at 1200 °C.

silicate systems are modelled with an error that is no larger than the maximum variation of 0.1 shown in Fig. 2.

An analysis of the NMR results reported by different authors for the compositions listed in Table 1 shows that, on the average, the uncertainty in the experimental measurements of Q^n values can be estimated as 10%, which is comparable with the above error of modelling. In the majority of cases given in the table, except for Q^3 in the composition $Li_2O \cdot 2SiO_2$, the maximum discrepancy between the model and experimental values of Q^n is noticeably less than 20%, i.e. the sum of the experimental error and the uncertainty of modelling. The larger deviation observed for Q^3 in the lithium disilicate glass is due to unreliable information concerning the thermodynamic potentials for lithium silicates reported in Refs. [18–21] and used

Table 2

Results from deconvolution of NMR spectra (attributed population of silicon species and center of each distribution of isotropic chemical shift values δ_{ISO}) and predictions of the TM

Glass	$Q^0 + Q^1$	Q^2	Q^3	Q^4
CS				
Central δ_{ISO} [ppm]	−75.6	−82.6	−91.8	−103.3
Population (NMR) [%]	$0 + (20 \pm 5)$	64 ± 8	14 ± 5	2 ± 1
Population (NMR) [%][a]	$0.7 + 19.3$	54.7	24.1	1.1
Population (TM) [%]	$1.9 + 25$	58.6	0	14.5
1·2·3				
Central δ_{ISO} [ppm]	−73.4	−80	−88.5	
Population (NMR) [%]	$0 + (16 \pm 5)$	72 ± 8	12 ± 5	
Population (TM) [%]	$5.0 + 4.6$	77	11.6	1.5
2·1·3				
Central δ_{ISO} [ppm]	−70.0	−77.5	−85.3	
Population (NMR) [%]	$0 + (14 \pm 5)$	67 ± 8	19 ± 5	
Population (TM) [%]	$4.5 + 1.3$	84	9.6	0.4
BS2				
Central δ_{ISO} [ppm]		−86.2	−93	−102.8
Population (NMR) [%]		24 ± 7	62 ± 5	14 ± 5
Population (TM) [%]	$0.007 + 0$	17.9	64	17.9
CMS2				
Central δ_{ISO} [ppm]	−77.5	−84.0	−92.7	−103.0
Population (NMR) [%]	$0 + (28 \pm 8)$	43 ± 10	25 ± 6	4 ± 1
Population (TM) [%]	$13.3 + 4.4$	67	0	15.6
PS				
4-Gaussian				
Central δ_{ISO} [ppm]	−79.3	−85.7	−94.4	−105.5
Population (NMR) [%]	$0 + (21 \pm 4)$	47 ± 8	26 ± 5	6 ± 2
Population (NMR) [%][b]	$0 + 12.8$	51	30	5.9
3-Gaussian				
Central δ_{ISO} [ppm]		−84.4	–	−94.8/−105.6
Population (NMR) [%][c]		73 ± 7	–	$22 \pm 5/5 \pm 2$
Population (TM) [%]	$1.5 + 0$	68.5	0	30

[a] Ref. [25].
[b] Ref. [26].
[c] Deconvolution with three Gaussian distributions of δ_{ISO}, and attribution of the Gaussians at −98.8 and −105.6 ppm to different Q^4 environments.

in the model calculations. Thus, it can be said that, for alkali-silicate glasses, the model results are in good agreement with the experimental values.

Before comparing the experimental and model Q^n values listed in Table 2 for the compositions $CaO \cdot SiO_2$ (CS), $BaO \cdot 2SiO_2$ (BS2), $Na_2O \cdot 2CaO \cdot 3SiO_2$ $(1 \cdot 2 \cdot 3)$, $2Na_2O \cdot CaO \cdot 3SiO_2$ $(2 \cdot 1 \cdot 3)$, $CaO \cdot MgO \cdot 2SiO_2$ (CMS2) and $PbO \cdot SiO_2$ (PS), it is necessary to consider the equations used, in each case, for calculating Q^n values on the basis of information about the chemical structure of the above glasses. It should be remembered that the sets of salt-like groupings, which characterise the chemical structure, are determined from an analysis of the phase diagram of the given system. For simplicity, binary glasses will be considered first.

4.1.1. $CaO \cdot SiO_2$ (CS)

According to the phase diagram of the system CaO–SiO_2 reported in Ref. [14], the groupings present in calcium silicate glasses include $CaO \cdot SiO_2$, $3CaO \cdot 2SiO_2$, $2CaO \cdot SiO_2$ and $3CaO \cdot SiO_2$ as well as the unreacted oxides SiO_2 and CaO. As follows from their stoichiometry and the structural data for the relevant crystalline compounds, these groupings bring into the glasses the following structural species: Q^2 ($CaO \cdot SiO_2$), Q^1 ($3CaO \cdot 2SiO_2$), Q^0 ($2CaO \cdot SiO_2$ and $3CaO \cdot SiO_2$) and Q^4 (SiO_2). As explained in Ref. [15], the model does not predict the presence of Q^3 in these glasses, since calcium disilicate, $CaO \cdot 2SiO_2$, which could introduce this species, is not shown in the phase diagram.

The model values of Q^n presented in Table 2 for the glass CS have been calculated using the equations given below. They establish the relationship between the content (fractions) of each Q^n species and the chemical structure of the glass:

$$Q^4 = \frac{X_{SiO_2}}{\sum Q^n},$$

$$Q^2 = \frac{X_{CaO \cdot SiO_2}}{\sum Q^n},$$

$$Q^1 = \frac{2X_{3CaO \cdot 2SiO_2}}{\sum Q^n},$$

$$Q^0 = \frac{X_{2CaO \cdot SiO_2} + X_{3CaO \cdot SiO_2}}{\sum Q^n},$$

where

$$\sum Q^n = X_{SiO_2} + X_{CaO \cdot SiO_2} + 2X_{3CaO \cdot 2SiO_2} + X_{2CaO \cdot SiO_2} + X_{3CaO \cdot SiO_2}.$$

Here and in what follows, the symbol $\sum Q^n$ represents the sum of all the structural species, while $X_{MO(M_2O) \cdot SiO_2}$ and X_{SiO_2} denote, respectively, the mole fractions of the salt-like groupings and the unreacted SiO_2 present in the glass considered.

4.1.2. $BaO \cdot 2SiO_2$ (BS2)

As follows from the phase diagram of the system BaO–SiO_2 [14], the chemical structure of barium silicate glasses is determined by the groupings $BaO \cdot 2SiO_2$, $2BaO \cdot 3SiO_2$, $BaO \cdot SiO_2$, $2BaO \cdot SiO_2$, and the unreacted oxides SiO_2 and BaO. They introduce into glasses the structural species Q^3 ($BaO \cdot 2SiO_2$ and $2BaO \cdot 3SiO_2$), Q^2 ($BaO \cdot SiO_2$ and $2BaO \cdot 3SiO_2$), Q^0 ($2BaO \cdot SiO_2$) and Q^4 (SiO_2). The content of these species in the glass BS2 is calculated using the relationships:

$$Q^4 = \frac{X_{SiO_2}}{\sum Q^n},$$

$$Q^3 = \frac{2X_{BaO \cdot 2SiO_2} + 2X_{2BaO \cdot 3SiO_2}}{\sum Q^n},$$

$$Q^2 = \frac{X_{BaO \cdot SiO_2} + X_{2BaO \cdot 3SiO_2}}{\sum Q^n},$$

$$Q^0 = \frac{X_{2BaO \cdot SiO_2}}{\sum Q^n},$$

where

$$\sum Q^n = X_{SiO_2} + 2X_{BaO \cdot 2SiO_2} + 3X_{2BaO \cdot 3SiO_2} + X_{BaO \cdot SiO_2} + X_{2BaO \cdot SiO_2}.$$

4.1.3. $PbO \cdot SiO_2$ (PS)

In the literature [14,22], two variants of the phase diagram are reported for the system PbO–SiO_2, according to which the sets of salt-like groupings present in the glass are somewhat different, viz $PbO \cdot SiO_2$, $2PbO \cdot SiO_2$ and $4PbO \cdot SiO_2$ [14], or $5PbO \cdot 8SiO_2$, $PbO \cdot SiO_2$, $2PbO \cdot SiO_2$, $3PbO \cdot SiO_2$ and $4PbO \cdot SiO_2$ [23]. In addition, in both cases, the unreacted oxides PbO and SiO_2 are also present. The groupings from the former set are responsible for the presence in the glasses of

the species Q^2 (PbO $\cdot$ SiO$_2$ and 2PbO $\cdot$ SiO$_2$), Q^0 (4PbO $\cdot$ SiO$_2$) and Q^4 (SiO$_2$), while the latter set yields a slightly larger variety of Q^n species, which comprises Q^3 (5PbO $\cdot$ 8SiO$_2$), Q^2 (5PbO $\cdot$ 8SiO$_2$, PbO $\cdot$ SiO$_2$ and 2PbO $\cdot$ SiO$_2$), Q^0 (3PbO $\cdot$ SiO$_2$ and 4PbO $\cdot$ SiO$_2$) and Q^4 (SiO$_2$). Special attention should be paid to the role of the grouping 2PbO $\cdot$ SiO$_2$. As follows from the experimental studies of lead silicate crystals [24], the structure of the compound 2PbO $\cdot$ SiO$_2$ gives raise to the species Q^2 and not Q^0, as could be expected from its stoichiometry. According to recent structural data [10], it is possible to assume a structural similarity between the crystals and salt-like groupings of the same stoichiometry. This enables an assumption to be made that the grouping 2PbO $\cdot$ SiO$_2$ brings into the glasses the species Q^2 instead of Q^0. It should also be noted that the difference in the chemical structure calculated on the basis of the two sets of lead silicate species is insignificant, due a small contribution from the groupings 5PbO $\cdot$ 8SiO$_2$ and 3PbO $\cdot$ SiO$_2$. Therefore, the model values Q^n given in Table 2 have been calculated using the smaller set of the groupings:

$$Q^4 = \frac{X_{SiO_2}}{\sum Q^n},$$

$$Q^2 = \frac{X_{PbO \cdot SiO_2} + X_{2PbO \cdot SiO_2}}{\sum Q^n},$$

$$Q^0 = \frac{X_{4PbO \cdot SiO_2}}{\sum Q^n},$$

where

$$\sum Q^n = X_{SiO_2} + X_{PbO \cdot SiO_2} + 2X_{2PbO \cdot SiO_2} + X_{4PbO \cdot SiO_2}.$$

4.1.4. $Na_2O \cdot 2CaO \cdot 3SiO_2$ $(1 \cdot 2 \cdot 3)$ and $2Na_2O \cdot 1CaO \cdot 3SiO_2$ $(2 \cdot 1 \cdot 3)$

In accordance with the phase diagrams of the ternary system Na$_2$O–CaO–SiO$_2$ [23] and its binary constituents, Na$_2$O–SiO$_2$ and CaO–SiO$_2$ [14], the chemical structure of sodium calcium silicate glasses is characterized by the presence of three unreacted oxides, Na$_2$O, CaO and SiO$_2$, and 16 salt-like species. The latter include 5 sodium silicates, 3Na$_2$O $\cdot$ 8SiO$_2$, Na$_2$O $\cdot$ 2SiO$_2$, Na$_2$O $\cdot$ SiO$_2$, 3Na$_2$O $\cdot$ 2SiO$_2$ and 2Na$_2$O $\cdot$ SiO$_2$, 4 calcium silicates, CaO $\cdot$ SiO$_2$, 3CaO $\cdot$ 2SiO$_2$, 2CaO $\cdot$ SiO$_2$ and 3CaO $\cdot$ SiO$_2$, and 7 sodium calcium silicates, Na$_2$O $\cdot$ 3CaO $\cdot$ 6SiO$_2$, Na$_2$O $\cdot$ 2CaO $\cdot$ 3SiO$_2$, 2Na$_2$O $\cdot$ CaO $\cdot$ 3SiO$_2$, Na$_2$O $\cdot$ CaO $\cdot$ SiO$_2$, Na$_2$O $\cdot$ 2CaO $\cdot$ 2SiO$_2$, 4Na$_2$O $\cdot$ 3CaO $\cdot$ 5SiO$_2$ and Na$_2$O $\cdot$ CaO $\cdot$ 5SiO$_2$. These groupings bring the following Q^n species into the glasses: Q^4 (SiO$_2$, 3Na$_2$O $\cdot$ 8SiO$_2$ and Na$_2$O $\cdot$ CaO $\cdot$ 5SiO$_2$), Q^3 (3Na$_2$O $\cdot$ 8SiO$_2$, Na$_2$O $\cdot$ 2SiO$_2$, Na$_2$O $\cdot$ 3CaO $\cdot$ 6SiO$_2$ and Na$_2$O $\cdot$ CaO $\cdot$ 5SiO$_2$), Q^2 (Na$_2$O $\cdot$ SiO$_2$, CaO $\cdot$ SiO$_2$, Na$_2$O $\cdot$ 3CaO $\cdot$ 6SiO$_2$, Na$_2$O $\cdot$ 2CaO $\cdot$ 3SiO$_2$, 2Na$_2$O $\cdot$ CaO $\cdot$ 3SiO$_2$ and 4Na$_2$O $\cdot$ 3CaO $\cdot$ 5SiO$_2$), Q^1 (3Na$_2$O $\cdot$ 2SiO$_2$, 3CaO $\cdot$ 2SiO$_2$, Na$_2$O $\cdot$ 2CaO $\cdot$ 2SiO$_2$ and 4Na$_2$O $\cdot$ 3CaO $\cdot$ 5SiO$_2$) and Q^0 (2Na$_2$O $\cdot$ SiO$_2$, 2CaO $\cdot$ SiO$_2$, 3CaO $\cdot$ SiO$_2$ and Na$_2$O $\cdot$ CaO $\cdot$ SiO$_2$). The content of these species in the glasses $1 \cdot 2 \cdot 3$ and $2 \cdot 1 \cdot 3$ is calculated from their chemical structure as

$$Q^4 = \frac{X_{SiO_2} + 2X_{3Na_2O \cdot 8SiO_2} + X_{Na_2O \cdot CaO \cdot 5SiO_2}}{\sum Q^n},$$

$$Q^3 = \frac{6X_{3Na_2O \cdot 8SiO_2} + 2X_{Na_2O \cdot 2SiO_2} + 4X_{Na_2O \cdot 3CaO \cdot 6SiO_2} + 4X_{Na_2O \cdot CaO \cdot 5SiO_2}}{\sum Q^n},$$

$$Q^2 = \frac{X_{Na_2O \cdot SiO_2} + X_{CaO \cdot SiO_2} + 2X_{Na_2O \cdot 3CaO \cdot 6SiO_2} + 3X_{Na_2O \cdot 2CaO \cdot 3SiO_2} + 3X_{2Na_2O \cdot CaO \cdot 3SiO_2} + X_{4Na_2O \cdot 3CaO \cdot 5SiO_2}}{\sum Q^n},$$

$$Q^1 = \frac{2X_{3Na_2O \cdot 2SiO_2} + 2X_{3CaO \cdot 2SiO_2} + 2X_{Na_2O \cdot 2CaO \cdot 2SiO_2} + 4X_{4Na_2O \cdot 3CaO \cdot 5SiO_2}}{\sum Q^n},$$

$$Q^0 = \frac{X_{2Na_2O \cdot SiO_2} + X_{2CaO \cdot SiO_2} + X_{3CaO \cdot SiO_2} + X_{Na_2O \cdot CaO \cdot SiO_2}}{\sum Q^n},$$

where

$$\sum Q^n = X_{SiO_2} + 8X_{3Na_2O \cdot 8SiO_2} + 2X_{Na_2O \cdot 2SiO_2}$$
$$+ X_{Na_2O \cdot SiO_2} + 2X_{3Na_2O \cdot 2SiO_2} + X_{2Na_2O \cdot SiO_2}$$
$$+ X_{CaO \cdot SiO_2} + 2X_{3CaO \cdot 2SiO_2} + X_{2CaO \cdot SiO_2}$$
$$+ X_{3CaO \cdot SiO_2} + 5X_{Na_2O \cdot CaO \cdot 5SiO_2}$$
$$+ 6X_{Na_2O \cdot 3CaO \cdot 6SiO_2} + 3X_{Na_2O \cdot 2CaO \cdot 3SiO_2}$$
$$+ 3X_{2Na_2O \cdot CaO \cdot 3SiO_2} + 5X_{4Na_2O \cdot 3CaO \cdot 5SiO_2}$$
$$+ 2X_{Na_2O \cdot 2CaO \cdot 2SiO_2} + X_{Na_2O \cdot CaO \cdot SiO_2}.$$

where

$$\sum Q^n = X_{SiO_2} + X_{CaO \cdot SiO_2} + 2X_{3CaO \cdot 2SiO_2}$$
$$+ X_{2CaO \cdot SiO_2} + X_{3CaO \cdot SiO_2} + X_{MgO \cdot SiO_2}$$
$$+ X_{2MgO \cdot SiO_2} + 2X_{CaO \cdot MgO \cdot 2SiO_2}$$
$$+ 6X_{5CaO \cdot 2MgO \cdot 6SiO_2} + 2X_{2CaO \cdot MgO \cdot 2SiO_2}$$
$$+ X_{CaO \cdot MgO \cdot SiO_2} + 2X_{3CaO \cdot MgO \cdot 2SiO_2}.$$

4.1.5. $CaO \cdot MgO \cdot 2SiO_2$ (CMS2)

From the phase diagrams of the ternary system CaO–MgO–SiO₂ [23] and its binary constituents, CaO–SiO₂ and MgO–SiO₂ [14], the chemical structure of calcium magnesium silicate glasses is determined by three unreacted oxides, CaO, MgO and SiO₂, and 11 salt-like groupings that include 4 calcium silicates, $CaO \cdot SiO_2$, $3CaO \cdot 2SiO_2$, $2CaO \cdot SiO_2$ and $3CaO \cdot SiO_2$, 2 magnesium silicates, $MgO \cdot SiO_2$ and $2MgO \cdot SiO_2$, and 5 calcium magnesium silicates, $CaO \cdot MgO \cdot 2SiO_2$, $2CaO \cdot MgO \cdot 2SiO_2$, $CaO \cdot MgO \cdot SiO_2$, $3CaO \cdot MgO \cdot 2SiO_2$ and $5CaO \cdot 2MgO \cdot 6SiO_2$. Due to the above groupings, the following structural species are present in the glasses: Q^4 (SiO_2), Q^2 ($CaO \cdot SiO_2$, $MgO \cdot SiO_2$, $CaO \cdot MgO \cdot 2SiO_2$ and $5CaO \cdot 2MgO \cdot 6SiO_2$), Q^1 ($3CaO \cdot 2SiO_2$, $2CaO \cdot MgO \cdot 2SiO_2$ and $5CaO \cdot 2MgO \cdot 6SiO_2$) and Q^0 ($2CaO \cdot SiO_2$, $2MgO \cdot SiO_2$, $3CaO \cdot SiO_2$, $CaO \cdot MgO \cdot SiO_2$ and $3CaO \cdot MgO \cdot 2SiO_2$). A knowledge of the chemical structure of the glass CMS2 enables the content of these species to be calculated using the following equations:

Note that, in all of the above equations, the numerical coefficients represent the numbers of silicon–oxygen tetrahedra of a given type in each of the salt-like groupings that bring this particular Q^n species to a glass. For the compositions listed in Table 2, practically all of these coefficients are determined on the basis of information on the structure of the relevant stoichiometric crystalline compounds.

It should be mentioned that the chemical structure of the glasses considered in this paper has been calculated using the standard Gibbs free energies of formation of the relevant crystals reported in Refs. [18–21]. All of the model values of Q^n have been determined at temperatures that differ from the respective glass transition temperatures, T_g, by less than 50°. From the above equations it follows that, even in the relatively simple binary glasses CS, BS2 and PS, some of Q^n species are introduced by two different salt-like groupings. As to more complex ternary glasses, all of their structural units, except for Q^4 in CMS2, are the result of several (3–6) groupings.

$$Q^4 = \frac{X_{SiO_2}}{\sum Q^n},$$
$$Q^2 = \frac{X_{CaO \cdot SiO_2} + X_{MgO \cdot SiO_2} + 2X_{CaO \cdot MgO \cdot 2SiO_2} + 4X_{5CaO \cdot 2MgO \cdot 6SiO_2}}{\sum Q^n},$$
$$Q^1 = \frac{2X_{3CaO \cdot 2SiO_2} + 2X_{2CaO \cdot MgO \cdot 2SiO_2} + 2X_{5CaO \cdot 2MgO \cdot 6SiO_2}}{\sum Q^n},$$
$$Q^0 = \frac{X_{2CaO \cdot SiO_2} + X_{3CaO \cdot SiO_2} + X_{2MgO \cdot SiO_2} + X_{CaO \cdot MgO \cdot SiO_2} + 2X_{3CaO \cdot MgO \cdot 2SiO_2}}{\sum Q^n},$$

4.2. NMR spectroscopy

4.2.1. CaO·SiO₂ (CS, wollastonite)

Fig. 3(a) shows plots of the experimental spectrum and the four-Gaussian functions fitted to it. Parameters obtained from this deconvolution are shown in Table 2. The Q^n populations calculated with the TM are in disagreement with those obtained by NMR. The fundamental discrepancy arises from the fact that Q^3 groupings are not expected from the TM analysis, but NMR results indicate the existence of these species ($14 \pm 5\%$). In our analysis, the Gaussian distribution centered at -92.5 ppm with FWHM of 11 ppm was attributed to Q^3 units. This interpretation was based on the identification of Q^4 resonances at -103.3 ppm and the fact that each NBO produces a deshielding of the silicon resonance of between $+5$ and $+10$ ppm.

Furthermore, 2-D NMR isotropic-anisotropic chemical shift correlation experiments in wollastonite glass support this attribution [25]. The authors of Ref. [25] observed that the *anisotropy* of the chemical shift interaction in the -92 ppm region does not correspond to Q^4 units, but is clearly related to Q^3. Also, the typical Q^4 anisotropy was observed for δ_{ISO} values around -101 ppm. Values for Q^n populations obtained in that study are also indicated in Table 2, and show reasonable agreement with the present data.

4.2.2. Na₂O·2CaO·3SiO₂ (1·2·3)

Fig. 3(a) shows plots of the experimental data and fitted distributions for this glass. The high resolution ²⁹Si-NMR spectrum of $1·2·3$ was deconvoluted into three-Gaussian functions, giving each of them the distribution of δ_{ISO} associated
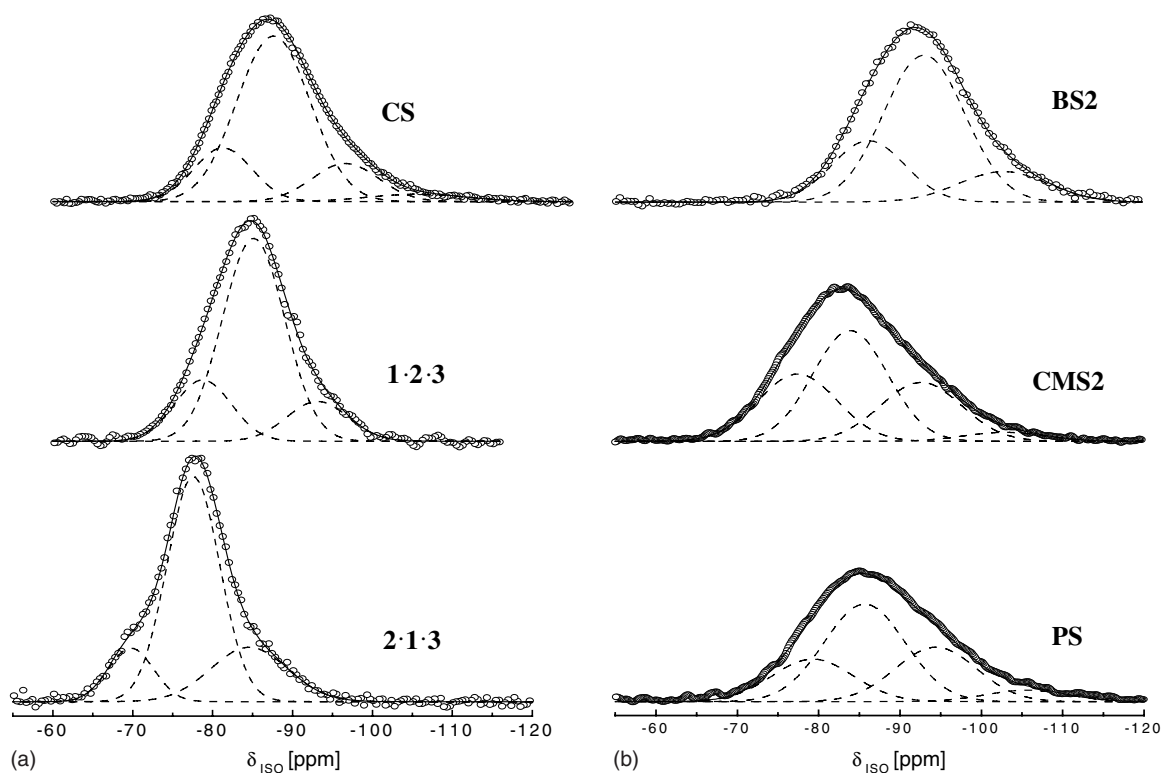

Fig. 3. (a) High resolution NMR spectra of the glasses CS, $1·2·3$ and $2·1·3$. Circles: experimental data. Dashed lines: Gaussian distributions of isotropic chemical shift for each silicon species, fitted by least-squares methods. Full line: resulting fit. (b) High resolution NMR spectra of the glasses BS2, CMS2 and PS. Circles: experimental data. Dashed lines: Gaussian distributions of isotropic chemical shift for each silicon species, fitted by least-squares methods. Full line: resulting fit.

with each type of silicon species Q^n. A remarkably stable deconvolution of the MAS–NMR spectrum was obtained, without imposing any physical constraint during the fitting. Table 2 shows the values extracted for the center of the δ_{ISO} distributions and the Q^n populations. Three kinds of silicon species were detected: Q^3, Q^2 and Q^1. A low concentration (<3%) of Q^0 species may be possibly included within the intensity fitted for Q^1 species, due to overlapping of chemical shift values. The populations show a remarkable agreement with the results of the TM.

4.2.3. $2Na_2O \cdot 1CaO \cdot 3SiO_2$ (2·1·3)

Fig. 3(a) shows that this glass has the best resolved spectrum of the set. Consequently, the deconvolution is stable and an excellent, unconstrained fit was obtained with three Gaussian functions for species attributed as Q^3, Q^2 and Q^1. The resulting parameters are shown in Table 2. A good agreement is observed with respect to the values predicted by TM, the greatest difference being that corresponding to the amount of $Q^0 + Q^1$ units.

4.2.4. $BaO \cdot 2SiO_2$ (BS2)

Fig. 3(b) shows that the NMR spectrum of this glass has no specially resolved features, aside from a high field asymmetry caused by Q^4 species. Thus, during the fitting procedure the FWHM of the three required Gaussians had to be constrained to 11 ± 1 ppm, a value typically observed in other silicate glasses. Under these conditions a unique fit was obtained, giving the set of populations shown in Table 2. These values are in good agreement with TM calculations. As can be observed, the maximum population corresponds to Q^3 sites, as expected for a disilicate composition.

4.2.5. $CaO \cdot MgO \cdot 2SiO_2$ (CMS2)

A deconvolution was performed with four Gaussian functions, to allow the presence of Q^4, Q^3, Q^2 and Q^1 species. The spectra and fitted distributions are plotted in Fig. 3(b), while the fit parameters are summarized in Table 2. As for wollastonite, the Q^n populations obtained by NMR disagree with the TM, especially in the attribution of Q^3 species. The TM excludes the presence of Q^3 species, but an intense distribution must be considered to account for the spectral intensity around −93 ppm.

4.2.6. $PbO \cdot SiO_2$ (PS, alamosite)

Fig. 3(b) shows that the NMR spectrum of this glass is very similar to CSM2. A deconvolution with four Gaussians was performed, resulting in the parameters shown in Table 2. Since Q^4 species are clearly present in this glass, as is evidenced from the NMR signal around −105 ppm, the other distributions are readily attributed to Q^3, Q^2 and Q^1 species. These results agree with a study of local order in lead silicate glasses presented in Ref. [26]. However, populations estimated by NMR are in disagreement with TM calculations, because in this glass the TM ruled out the presence of Q^3 species, as in CMS2 and CS.

5. Discussion

As mentioned above, there is a common disagreement between TM and NMR estimations of the populations Q^n in the glasses CS, CMS2 and PS. There are no crystalline compounds in the phase diagram of these systems having Q^3 units, but the analysis of their NMR spectra suggest the presence of these species. The identification of Q^3 in the spectra is based on the following argument: in silica polymorphs, there are no effects on the δ_{ISO} value arising from the neighborhood of network modifying cations nor from covalent bonds other than Si–O. Therefore, δ_{ISO} is determined basically by the mean value of the Si–Ô–Si angle [17]. In a glassy silica sample, the total range spanned by δ_{ISO} is from −100 to −125 ppm. These limits are determined by the distribution of possible Si–Ô–Si angles, varying from 120° to 180° [27]. The maximum of the silica glass spectrum is around −111 ppm and corresponds to a mean Si–Ô–Si angle of 146°. Considering this fact, distributions of δ_{ISO} centered between −91 and −94 ppm, as observed in CS, CMS2 and PS glasses, could hardly be attributed to Q^4 sites. Instead, distributions centered between −103 and −106 ppm were observed for these glasses, which can be readily attributed to Q^4 species. Therefore, the less

shielded distributions between −91 and −94 ppm should correspond to Q^3, since their difference in mean δ_{ISO} with respect to Q^4 agrees with the expected deshielding produced by one NBO.

On the other hand, in the context of the TM, it is difficult to associate these Q^3 populations with chemical structures not considered in the calculations, since these structures should be related to crystalline phases not yet observed in the equilibrium phase diagrams.

It should be noted that the set of chemical structures (the salt-like groupings or species, as they are called in the thermodynamic approach), as determined by the relevant phase diagram, is strictly specific for each particular system. Its choice should receive very careful attention, because neglecting even a single compound that forms in a given system makes it impossible to correctly model its thermodynamic potentials. Since these potentials are a function only of the chemical structure of a glass or melt, modelling their value presents the most direct and reliable test for checking the correctness of a chosen set of salt-like species. This is illustrated by Fig. 4, which shows the chemical potential of Na_2O in sodium silicate melts, at 1200 °C, modelled using different sets of species. It is seen that neglecting the formation of $Na_2O \cdot 2SiO_2$ considerably changes the
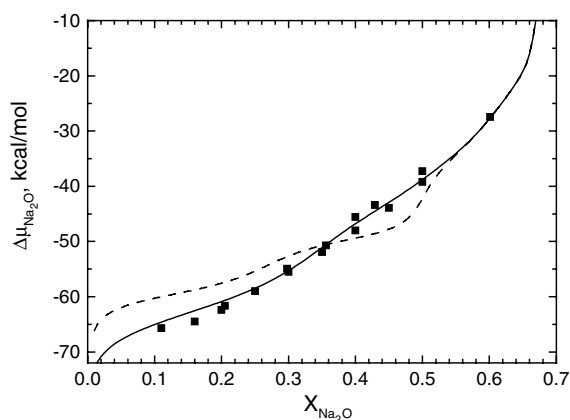
shape of the model curve. Only by taking into account the complete set of species, an agreement with the experimental data can be obtained [1].

Fig. 5 shows the results of modelling the chemical potential of Na_2O in sodium calcium silicate melts. It is seen that, in the cuts with the ratio $Na_2O/(Na_2O + SiO_2)$ equal to 0.244 and 0.294, the deviation between the model values and the experimental data [28] does not exceed 0.5 kcal/mol, which can be considered as good agreement. At $Na_2O/(Na_2O + SiO_2) = 0.343$, this deviation is larger (up to 1 kcal/mol), which is due to an insufficient accuracy in the experimental data for this cut. Hence it can be concluded that, in terms of thermodynamics, the set of the salt-like species in sodium calcium silicate glasses has been chosen correctly. Therefore, another possibility should be considered in order to explain the origin of the observed Q^3 silicon for these compositions.

It should be noted that TM calculations provide the concentration of salt-like and starting oxides species. The populations of Q^n units in the glass are calculated from these quantities considering the type of Q^n existing in each chemical compound, assuming they have structures similar to those observed in crystalline samples. For CS, CMS2 and PS glasses, the calculated concentration of silica provides the fraction of Q^4 units in

Fig. 4. Chemical potential $\Delta\mu$ of Na_2O in sodium silicate melts, at 1200 °C, modelled using different sets of species. Squares: experimental data (Ref. [1]). Solid line: calculations considering all salt-like compounds. Dashed line: calculations neglecting $Na_2O \cdot 2SiO_2$.
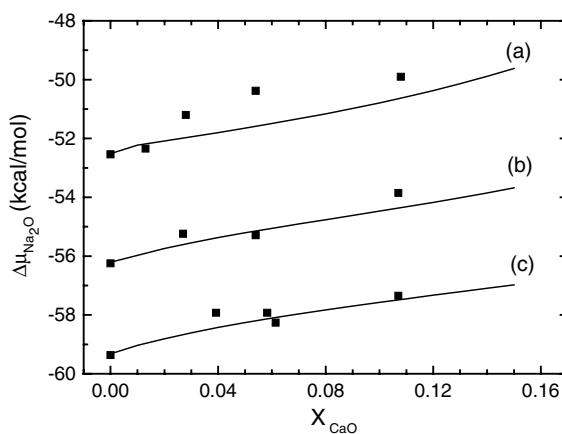

Fig. 5. Chemical potential $\Delta\mu$ modelled for Na_2O in sodium calcium silicate melts. Solid lines: calculations for different values of the ratio $Na_2O/Na_2O + SiO_2$: (a) 0.343, (b) 0.294, (c) 0.244. Squares: Neudorf's experimental data (Ref. [28]).

the glass, assuming that these Q^4 species are organized as in a bulk silica crystal. Nevertheless, it is well known that this is not the case for silica in highly dispersed forms, such as nano-particles or highly porous media. In these forms, the surface to volume ratio could be high enough that Q^3 groups on the interface can be detected with ^{29}Si-NMR. Many well established observations of silicon species on the surface of silica can be found in literature for different types of dispersed silica (e.g. Ref. [17], Chapter V and references therein; Ref. [29, p. 212]). Hence, we propose that the amount of silica-like units predicted by the TM for CS, CMS2 and PS glasses correspond to silica-like (Q^4) domains of molecular dimensions, where an appreciable amount of Q^3 units should necessarily exist on the 'surface'. In this way, the population of Q^3 units detected by NMR in these glasses should be attributed to these molecular size silica-like domains, instead of another salt-like compound.

Following this interpretation, the amount of silicon corresponding to silica-like domains should be calculated as the sum of silicon populations detected by NMR in Q^3 and Q^4 sites. This is the experimental quantity that should be used in comparisons with populations calculated with the TM. These quantities are summarized in Table 3. With this new interpretation, a reasonable agreement is found between the sum of Q^3 and Q^4 populations from NMR and the fraction of silicon in silica-like clusters predicted by the model for glasses CS and PS. The agreement is not so close for CMS2 (NMR: 29 ± 7%, TM: 15.6%). However, this glass has the broadest spectrum of the

glasses studied and a strong overlap exists among the fitted distributions. This fact constitutes a limitation in resolving the details of the δ_{ISO} distribution arising from the silica domains. Accordingly, the number of fitted parameters can be reduced by considering only a single broad distribution for silica, covering δ_{ISO} values from Q^3 and Q^4. In this case, resulting the silica population is 24 ± 7; a value closer to the estimation of the model. On the other hand, it should be noted that, in glasses $1 \cdot 2 \cdot 3$ and $2 \cdot 1 \cdot 3$, the expected amount of silica from TM (1.5% and 0.4%, respectively) is below the sensitivity threshold for NMR. Therefore, any possible effects due to finite-size silica clusters modifying the values for Q^3 populations could not be measured in these glasses.

Regarding the BS2 glass, the only disilicate glass of the set, substantial amounts of Q^3 and Q^4 are expected from the model calculations: 17.9% and 64%, respectively. The Q^3 and Q^4 populations determined from NMR agree quite well with the TM values. No excess of Q^3 units (with respect to the calculations) was observed within the experimental uncertainty. In this case, the silica-like domains in BS2 should have a low surface to volume ratio, giving a negligible contribution to the total population of Q^3 sites.

6. Conclusions

The relative content of Q^n groups species in six stoichiometric glasses has been calculated using the model of associated solutions and compared

Table 3
Population of silicon species considering finite-size silica domains (having Q^3 and Q^4 units) in glasses where Q^3-bearing compounds are not expected from thermodynamics modeling

Glass	$Q^0 + Q^1$	Q^2	Q^{silica} ($Q^3 + Q^4$)
CS			
Population (NMR) [%]	20 ± 5	64 ± 8	16 ± 6
Population (TM) [%]	$1.9 + 25 = 26.9$	58.6	14.5
CMS2			
Population (NMR) [%]	16 ± 8	60 ± 10	24 ± 7
Population (TM) [%]	$13.3 + 4.4 = 17.7$	66.6	15.6
PS			
Population (NMR) [%]	–	73 ± 7	27 ± 7
Population (TM) [%]	$1.5 + 0$	68.5	30

with NMR measurements for six glasses. Satisfactory agreement was found between the predicted and experimental Q^n populations for glasses $1 \cdot 2 \cdot 3$, BS2 and $2 \cdot 1 \cdot 3$. The apparent disagreement with respect to the experimental data of Q^3 units in three glasses of the set (CS, CMS2, PS) can be accounted for by considering the finite-size of the Q^4 groupings species in the network. If it is assumed that the expected amount of Q^4 silicon in the glass is organized in silica-like domains of molecular size, which thus have Q^3 units at their 'interfaces', the model predictions are consistent with experimental the data. Therefore, within the overall uncertainty of the experimental method and calculations, the content of Q^n species predicted by the model is in satisfactory agreement with the results of NMR experiments. This fact indicates that thermodynamic modeling is a useful tool in predicting structural aspects of glass.

Acknowledgements

References

[1] B.A. Shakhmatkin, N.M. Vedishcheva, J. Non-Cryst. Solids 171 (1994) 1.

[2] B.A. Shakhmatkin, N.M. Vedishcheva, M.M. Shultz, A.C. Wright, J. Non-Cryst. Solids 177 (1994) 249.

[3] N.M. Vedishcheva, B.A. Shakhmatkin, M.M. Shultz, A.C. Wright, J. Non-Cryst. Solids 196 (1996) 239.

[4] B.A. Shakhmatkin, N.M. Vedishcheva, A.C. Wright, in: A.C. Wright, S.A. Feller, A.C. Hannon (Eds.), Borate Glasses, Crystals and Melts, Soc. Glass Techn, Sheffield, 1997, p. 189.

[5] B.A. Shakhmatkin, N.M. Vedishcheva, A.C. Wright, in: Proc. Intern. Congr. Glass, vol. 1, Invited Papers, Soc. Glass Techn, Sheffield, 2001, p. 52.

[6] B.A. Shakhmatkin, N.M. Vedishcheva, M.M. Shultz, A.C. Wright, Glass Sci. Technol. Glastechn. Ber. 67C (1994) 191.

[7] N.M. Vedishcheva, B.A. Shakhmatkin, M.M. Shultz, A.C. Wright, in: A.C. Wright, S.A. Feller, A.C. Hannon (Eds.), Borate Glasses, Crystals and Melts, Soc. Glass Techn., Sheffield, 1997, p. 215.

[8] N.M. Vedishcheva, B.A. Shakhmatkin, A.C. Wright, Fundamentals of Glass Science and Technology 1997, Glafo, Glass Res. Inst, Vaxjo, Sweden, 1997, p. 664.

[9] Th. De Donder, P. Van Rysselberghe, Thermodynamic Theory of Affinity, Stanford Univ., Stanford, CA, 1936, Translated under the title: Termodinamicheskaya teoriya srodstva, V.M. Glazov (Ed.), Metallurgiya, Moscow, 1984.

[10] A.C. Wright, N.M. Vedishcheva, B.A. Shakhmatkin, in: C.A. Angell, K.L. Ngai, J. Kieffer, T. Egami, G.U. Nienhaus (Eds.), Structure and Dynamics of Glasses and Glass Formers, Mater. Res. Soc. Symp. Proc., Pittsburgh, PA, vol. 455, 1997, p. 381.

[11] A.M. Evseev, L.S. Nikolaeva, Matematicheskoye modelirovaniye khimicheskikh ravnovesii (Mathematical modelling of chemical equilibria), Mosk. Gos. Univ., Moscow, 1988.

[12] S. Srikanth, K.T. Jacob, Metall. Trans. B 19 (1988) 465.

[13] I. Progogine, R. Defay, Chemical Thermodynamics, Longmans, London, 1954, Translated under the title: Khimicheskaya termodinamika, V.A. Mikhailov (Ed.) Nauka, Novosibirsk, 1966.

[14] N.A. Toropov, V.P. Barzakovskii, V.V. Lapin, N.N. Kurtseva, in: N.A. Toropov (Ed.), Diagrammy Sostoyaniya Silikatnykh Sistem (Phase Diagrams of Silicate Systems), vol. 1, Nauka, Leningrad, 1969 (in Russian).

[15] N.M. Vedishcheva, B.A. Shakhmatkin, A.C. Wright, J. Non-Cryst. Solids 293–295 (2001) 312.

[16] J. Schneider, V.R. Mastelaro, H. Panepucci, E.D. Zanotto, J. Non-Cryst. Solids 273 (2000) 8.

[17] G. Engelhardt, D. Michel, High Resolution Solid-State NMR of Silicates and Zeolites, John Wiley, Norwich, 1987.

[18] W.T. Thompson, A.D. Pelton, C.W. Bale, F*A*C*T-Web, Facility for the Analysis of Chemical Thermodynamics', Thermfact, 1998.

[19] I. Barin, O. Knacke, Thermodynamic Properties of Inorganic Substances, Springer, Berlin, 1973.

[20] M.W. Chase, C.A. Davis, J.R. Downey, D.J. Frurip, R.A. McDonald, A.N. Sywerud, JANAF Thermochemical Tables, 3rd Ed., American Chemical Society, American Institute of Physics, National Bureau of Standards, 1985.

[21] I. Barin, Thermochemical Data of Pure Substances, 2nd Ed., VCH, Weinheim, 1993.

[22] F.Ya. Galakhov (Ed.), Diagrammy Sostoyaniya Sistem Tugoplavkikh Oksidov (Phase Diagrams of Refractory Oxide Systems), Part 1, vol. 5, Nauka, Leningrad, 1985 (in Russian).

[23] N.A. Toropov, V.P. Barzakovskii, V.V. Lapin, N.N. Kurtseva, A.I. Boikova, in: V.P. Barzakovskii (Ed.), Diagrammy Sostoyaniya Silikatnykh Sistem (Phase Diagrams of Silicate Systems), vol. 3, Nauka, Leningrad, 1972 (in Russian).

[24] C. Bessada, D. Massiot, J. Coutures, A. Douy, J.P. Coutures, F. Taulelle, J. Non-Cryst. Solids 168 (1994) 76.

[25] P. Zhang, P. Grandinetti, J. Stebbins, J. Phys. Chem. B 101 (1997) 4004.

[26] F. Fayon, C. Bessada, D. Massiot, I. Farnan, J.P. Coutures, J. Non-Cryst. Solids 232 (1998) 403.

[27] R. Mozzi, B. Warren, J. Appl. Crystallogr. 2 (1969) 164.
[28] D.A. Neudorf, M.S. thesis, Massachusetts Institute of Technology, Cambridge, MA, 1979.
[29] H. Eckert, Prog. NMR Spectrosc. 24 (3) (1992) 159.
[30] Maekawa et al., J. Non-Cryst. Solids 127 (1991) 53.
[31] Emerson et al., J. Non-Cryst. Solids 113 (1989) 253.